LMSC F254276

Compton Gamma Ray Observatory/BATSE Observations of Energetic Electrons Scattered by Cyclotron Resonance with Waves from Powerful VLF Transmitters

Final Report

For the Compton Gamma Ray Guest Investigation Program

NASA Goddard Space Flight Center

Contract Number

NAS5-32065

Dayton W. Datlowe and William L. Imhof

Lockheed Palo Alto Research Laboratories

3251 Hanover Street, O/ 91-20 B 255

Palo Alto, California 94304

12 February 1994

Table of Contents

Compton Gamma Ray Observatory/BATSE Observations of Energetic Electrons Scattered by Cyclotron Resonance with Waves from Powerful VLF Transmitters

Dayton W. Datlowe and William L. Imhof

Lockheed Palo Alto Research Laboratories

Abstract

To obtain a better understanding of the wave-particle mechanisms responsible for the loss of electrons from the radiation belts, we have studied energetic electron data from the Burst and Transient Source Experiment (BATSE) on the NASA's Compton Gamma Ray Observatory (GRO). Powerful ground-based VLF transmitters resonantly scatter electrons from the inner radiation belt onto trajectories from which they precipitate into the atmosphere as they drift eastward. We have identified 563 instances in which the satellite traversed a cloud of energetic electrons which had been scattered into quasi-trapped trajectories. From the longitude distribution we conclude that waves from the VLF transmitter NWC at 114°E are the origin of 257 of the events, and waves from UMS at 44°E related to 45 more. In another 177 cases the electrons had drifted from the longitude of these transmitters to a location in the western hemisphere. The previously reported seasonal variation in the frequency of occurrence of cyclotron resonance interaction is confirmed with the continuous coverage provided by GRO. The frequency of occurrence of the cyclotron resonance interactions is largest before sunrise, which we attribute to the diurnal variations in the transmission VLF waves through the ionosphere. We also report for the first time unique very narrow sheets of electrons occurring in the aftermath of a large geomagnetic storm.

February 10, 1994

Compton Gamma Ray Observatory/BATSE Observations of Energetic Electrons Scattered by Cyclotron Resonance with Waves from Powerful VLF Transmitters

D. W. Datlowe and W. L. Imhof

Introduction

Precipitation of energetic electrons from the inner radiation belt in narrowly peaked spectra has been observed by a number of satellites. In a series of spectra recorded by a single satellite the energy of the peaks varies with L-value in a characteristic way, according to the condition for cyclotron resonance [*Brice*, 1964] with waves at a single VLF frequency. Since the cyclotron resonance condition is met, and because the peaks observed at satellite nighttime cluster around particular VLF transmitters [*Datlowe and Imhof*, 1990], the peaks are interpreted as the result of cyclotron resonance with VLF waves from ground based transmitters [*Inan et al.*, 1984].

Six different satellite experiments have reported data on cyclotron resonance precipitation of electrons. The first reports of the phenomenon were based on observations from P71-2 and P72-1 [*Imhof, Gaines, and Reagan*, 1973, 1974]. Later *Vampola and Kuck* [1978] reported observations from the OV1-14 and OV1-19 satellites. Further results came from S3-3 [*Vampola*, 1987] and P78-1 [*Imhof et al.*, 1981]. These papers are in general agreement that pitch angle scattering by waves from ground based transmitters is the most likely origin of the peaks, but reached differing conclusions as to the relative importance of various known stations. A large number of cyclotron resonance events were observed by the S81-1 satellite [*Datlowe and Imhof*, 1990] in the inner magneto-

sphere at altitudes between 170 and 270 km.. A map of the locations of 361 night time S81-1 events strongly favors the conclusion that one particular station, NWC in Australia, is a major contributor to the precipitation. The station is a communication transmitter located at 21°49′S and 114°10′ E, radiating 1000 kW at a frequency of 22.3 kHz [*Inan et al.* 1984]. All of the 221 cyclotron resonance events from the P78-1 experiment [*Datlowe and Imhof*, 1993] were observed in the vicinity of NWC in Australia or were on the trajectories of electrons that drift eastward from that site. S81-1 also frequently observed precipitation in the vicinity of NAA (17.8 kHz) and NSS (21.4 kHz) in the eastern United States. Electrons of 16 kev and 25 keV that were precipitated by waves from these stations were measured on a rocket flight from Wallops Island [*Arnoldy and Kintner,* 1989].

A seasonal variation in the median energy of the observed peaks was found by *Imhof et al.* [1978] in the period from November 1971 to August 1972; the energies of the peaks were reported to be lower in the summer months. The data from OV1-19 reported by *Vampola and Kuck* [1978] showed a sharp decrease in the number of observations in which cyclotron resonance effects were observed after day 270 of 1969. Plotting the S81-1 data in the same format, *Datlowe and Imhof* [1990] showed that the peaks in the eastern hemisphere (over NWC) were found mainly from May to September 1982, while peaks from stations in the western hemisphere were observed primarily after September. They used the term"Seasonal Variation", although the data covered only seven months. The same authors found further evidence for a seasonal variation came from a study of P78-1 data acquired over the five year span from March 1979 to July

1984. They further concluded [*Datlowe and Imhof*, 1993] that the origin of the seasonal variation was a change in the ionospheric transmission of VLF waves. Unfortunately the P78-1 data coverage was quite sparse after the first year of operations, so that the effect could only be inferred on a statistical basis.

Several features of the process in which waves from ground based VLF transmitters precipitate of inner belt electrons are not well understood. It is important to establish the relative contribution of various powerful transmitters to the overall precipitation rate and to learn what is unique about the few that dominate the process. The effectiveness of VLF transmitters in precipitating electrons is known to be greater at nighttime, but the local time dependence is not well known, in part because sun-synchronous satellites have provided much of the previous data. Evidence for seasonal effects has been previously presented but more detailed knowledge of the seasonal variation is required to understand the mechanism. The BATSE experiment has several features which are suitable for addressing these problems: very high sensitivity, continuous data coverage, and appropriate measurements at all local times. In this investigation we have used data from the first 11 months of the BATSE experiment to address these problems.

Instrumentation

The Compton Gamma-Ray Observatory (GRO) was designed to be the next major step in gamma-ray astronomy, by making high sensitivity measurements over the entire celestial sphere over six decades in energy, from 30 keV to 30 Gev. The 35,000 pound payload was launched in the Space shuttle and deployed by the astronauts in April,

1991. The satellite was launched into a 450 km circular orbit at 28.5° inclination. During the first 11 months of operations data were stored on tape recorders and 100% data coverage was obtained; later data were returned by the Tracking and Data Relay Satellite System (TDRSS) and about 65% data coverage was obtained. In this paper we will be using data from the time period, 28 April 1991 to 28 March 1992.

This investigation is based on data from the Burst and Transient Source Experiment (BATSE) on GRO. The primary objective is to study gamma-ray bursts, brief transients of x-ray emission from objects at astronomical distances. Since the bursts can occur at any time and appear from any direction, the BATSE monitors as much of the celestial sphere as possible. BATSE consists of 8 identical modules arranged in the geometry of an octahedron and placed on the corners of the spacecraft. Each main detector is a 20 inch diameter disk of sodium iodide scintillator which is 0.5 inches thick. The light is collected by three 5 inch diameter photomultiplier tubes. On the front of each main detector is a plastic anticoincidence shield and aluminum aperture which will absorb incoming electrons below 300 keV; however a small fraction ($<10^{-3}$) will produce x-rays which are recorded. The primary data for this investigation consist one second accumulations of the counting rate in each of the 8 x-ray detectors above 4 threshold energies: of 25, 50, 100, and 300 keV. To distinguish it from BATSE data with other spectral or time resolutions, the computer data files are often labelled "DISCLA". Although the spacecraft returned data continuously, the Large Area Detectors were routinely turned off in the vicinity of the South Atlantic Anomaly.

To detect cosmic gamma-ray bursts from any direction, BATSE has eight identical

faces arranged at the corners of an octahedron . A point source of X-rays will illuminate from one to four faces of the octahedron. The location of the burst can be inferred from the orientation of the satellite and the ratios of intensities on each face. The accuracy of the source location depends on the counting statistics, and may in practice be 1° in some cases. The technique has been used to find the distribution of cosmic x-ray sources [*Fishman et al.* , 1993].

Cyclotron Resonance Precipitation

The first order cyclotron resonance condition [*Brice*, 1964] is given by the equation

$$\omega - \mathbf{k}\cdot\mathbf{v} = \Omega/\gamma \qquad (1)$$

where ω is the VLF wave angular frequency, $\mathbf{k}$ is the VLF wave vector in the interaction region, $\mathbf{v}$ is the electron velocity vector, Ω is the electron cyclotron angular frequency, and γ is the relativistic factor. Evaluation of the wave vector $\mathbf{k}$ introduces the wave normal angle and the index of refraction. We calculate the index of refraction from the transmitter frequency, the cyclotron frequency, and the equatorial plasma density using the formulation of *Koons et al.* [1981]. The equatorial magnetic field is calculated from the model of *Olsen and Pfitzer* [1974] and the equatorial plasma density is calculated from the model of *Chiu et al.* [1979]. The equatorial pitch angle, a factor in the resonance condition, is calculated from the ratio of the local magnetic field to the equatorial magnetic field as given by the Olsen-Pfitzer model for the latitude, longitude, and altitude of the satellite at the time of the observation. Since our observations are made at low altitude and not in the equatorial interaction region, the wave normal angle cannot be observed directly and in our calculations we have assumed propagation

parallel to the magnetic field lines. The sensitivity of our calculation to changes in the assumptions is discussed in *Datlowe and Imhof* [1989]. Some of the previously cited papers have used different assumptions about the plasma density and wave propagation angle but have obtained comparable resonant energy values nonetheless.

Cyclotron resonance effects are most often observed at an L-value near L=1.65. At this magnetic L-value, electrons which are mirroring above the atmosphere at 200 km altitude have equatorial pitch angles ranging from 21.1° to 32.6°. The longitude dependance shown in Figure 1 is a consequence of the fact that the geomagnetic dipole is offset from the geocenter. On the time scales of interest here, both the L-value and the equatorial pitch angle are constants of the electron motion, but the electrons drift eastward at the rate of order ~3.6° per minute. Electrons with equatorial pitch angles greater than 32.6° will drift around the earth in stably trapped orbits. Electrons with equatorial pitch angles between 21.1° and 32.6° will drift eastward and be lost into the earth's atmosphere at altitudes of the order of 200 km. Since the lifetime of these electrons is very short, the background energetic electron flux is quite low. Accordingly at L=1.65 the gradient of energetic electron flux is large at 33° pitch angle and a small amount of pitch angle scattering will make a large change in the flux observed by a satellite below the stably trapped orbits. In contrast , a satellite above the 33° limit would need to detect a small energy dependent change in the pitch angle distribution to look for the effect. Electrons with equatorial pitch angles less than 21° will be absorbed by the atmosphere within a few bounce periods (seconds).

One of the results of the previous work summarized in *Datlowe and Imhof* [1990]

is that cyclotron resonance precipitation of electrons is only observed when the transmitter is in darkness. The day-night effect is understood to be due to increased attenuation of VLF waves by the ionosphere during daylight. Peaks from transmitter precipitation may be observed at locations which are in daylight, but all evidence is consistent with the fact that these electrons have drifted from a transmitter site which is in darkness. The effect is important when we try to identify a transmitter which is responsible for scattering electrons into quasi-trapped orbits, as the search is automatically narrowed to transmitters in darkness at that time (minus the drift time).

BATSE Measurements of Geomagnetically Trapped Electrons

In a cosmic x-ray burst, at most four faces of the BATSE instrument are illuminated at one time. The experiment also commonly observes events in which all eight faces are recording counts and opposite faces have the same counting rates. Electrons which are trapped in the geomagnetic field spiral about magnetic field lines. If their mirror point is comparable to the altitude of the satellite, the fluxes in opposite directions will be equal. Thus we infer that events seen in all eight detectors are due to fluxes of locally trapped electrons. Although electrons with energies below 300 keV cannot penetrate windows over the scintillation counters, they produce x-rays as they stop in the window material. The X-ray production above a given pulse-height threshold depends strongly on the electron spectrum, but the efficiency is of the order $\sim 10^{-3}$ [*Berger and Seltzer,* 1964]. With a collecting area over 10^4 cm^2, the geometric factor for electrons is of order of 1 cm^2 sr^{-1}.

To distinguish x-ray emission from a point source from locally trapped electrons, we

use the fact that the difference between opposite faces is a maximum for an x-ray source, while the difference between opposite faces is a minimum for locally trapped electrons. Figure 2 is an example of an electron event, showing counting rate data from one GRO orbit versus geographic longitude on 24 June, 1991. The upper trace is the sum of the eight counting rates above 50 keV. The lower traces is computed from the differences in the counting rates in opposite faces R_n and R_{7-n} as follows:

$$\sigma = \frac{\sqrt{\sum_0^3 (R_n - R_{7-n})^2}}{\sum_0^7 R_n} \qquad (1)$$

If all 8 faces have the same counting rate, σ is zero; if four faces sharing a common vertex are equally illuminated, σ =0.5; if only one face is illuminated, σ = 1. It is evident from the minimum in the lower trace in the Figure that the flux is equal on opposite faces and therefore we infer that locally trapped electrons are the source of the counts. At the time of maximum flux the satellite was at longitude 144°E and a latitude of 24°S; in geomagnetic coordinates it was at L=1.61.

Two encounters with energetic electrons on the same orbit, as shown in Figure 3, is another common case. The first peak at 132°E was observed in the southern hemisphere at L=1.68; the second peak at 251°E was observed in the northern hemisphere at L=1.66. These electrons have been pitch angle scattered by the same source of VLF waves; in the first peak they have drifted eastward ~18° (in ~ 10 minutes) from the transmitter to the point where the satellite crossed L=1.68; in the second case they have drifted 137° (in 72 minutes) to the point of observation.

Auroral and Solar x-ray Events

The BATSE experiment also detects strong x-ray emission from both solar and auroral emission. The x-ray events are readily distinguished from electron events by an increase in the parameter σ, because a limited number of faces are illuminated. Auroral emission occurs at high latitude over regions thousands of kilometers long and the emission is often stable in time. Figure 4 gives two typical examples of auroral x-ray events. On the left BATSE is detecting x-rays above 50 keV from the day side of the southern auroral zone at a magnetic local time of 14 hours. On the right BATSE is recording x-rays from the night side of the northern auroral zone at a magnetic local time of 2 hours. The smooth shape of the southern hemisphere x-ray counts is determined by the rising and the setting of the auroral zone in the field of view as GRO approaches and recedes from the southernmost excursion. The same effect modulates the recorded flux from the northern auroral zone as GRO approaches it northernmost excursion. In the first 11 months of BATSE data we identified 376 auroral events.

Solar hard x-ray emission is easily distinguished from auroral emission by its very impulsive nature. Figure 5 shows a typical solar flare event. The multiple spikes and impulsive rise in this event are often observed from solar flares. Since solar x-ray emission regions are for the current purposes point sources (angular size ~10 arc sec) the σ parameter is quite large. Auroral and trapped electron events are observed in consistent geographic locations which provide clues as to the origin of an event, but flares are observed at all latitudes and longitudes as long as the satellite is in daylight. The GOES solar x-ray catalog can also be used to confirm the solar origin of an event.

We have not made a count of solar x-ray flares as the definitive catalog is kept by the GRO solar flare team.

BATSE is an experiment to study emission from sources at astronomical distances, and as such the signals from terrestrial sources are a form of interference or background. Figure 6 illustrates the nature of the problem, showing successively an auroral event, a cosmic x-ray burst, and a cloud of energetic electrons precipitated by cyclotron resonance. Because we have used two second averages and summed all 8 detectors, the signal to noise ratio of the cosmic x-ray burst is degraded in this display. Nonetheless the Figure serves to illustrate that the signals from terrestrial effects may be quite large compared to signal from astronomical sources in the energy range 25-300 keV

Summary of the Electron Precipitation Events

We have identified 563 cyclotron resonance precipitation events in our survey of the first 11 months of BATSE data. In geographic coordinates these events occur in two zones: between 30° and 150° East longitude in the northern hemisphere and between 220° and 275° East in the southern hemisphere. Figure 7 shows a geographic map of the locations of the events. The map has been divided into bins of 5° longitude by 5° latitude and the number of events in each bin is designated with a gray-scale. The largest number is 73 events in the range 115°E - 120°E and 25°S - 30°S. The peaks in the electron flux occurred at L-values ranging from 1.40 to 1.86, with a median value of 1.69. The Figure shows two contours corresponding to L=1.65 at the altitude of the satellite, and the locations of several major VLF transmitter are also marked.

The fact that these events consist of electrons scattered to quasi-trapped pitch angles is illustrated by Figure 8. To make the pitch angle comparison meaningful the range of L-values has been restricted to 1.60 to 1.70. The Figure shows the equatorial pitch angle of 189 events as a function of geographic longitude. It is evident that all but a few events involve pitch angles less than the 32.6° limit of stable trapping. As in Figure 1, the pitch angle of electrons mirroring at the top of the atmosphere is indicated by solid and dashed lines; however plotted only at those longitudes when L=1.65 is below 28.5 latitude and is therefore reachable by the satellite. The Figure shows that there is a strong correlation between the occurrence of the events and the locations where the satellite is at or above L=1.65. If the inclination of the GRO orbit were as low as 24° the satellite would not reach L=1.65 and the frequency of resonance precipitation events would be greatly reduced.

The intensity of the resonance events is also strongly modulated by the precession of the plane of the orbit. Figure 9 shows the intensities of 563 cyclotron resonance peaks as a function of time. The orbital plane of GRO precesses around the earth-sun line with a period of about 45 days; this is about the same as the spacing between the peaks in Figure 9. The largest intensities in Figure 9 occur when the satellite is in the L=1.65 zone of maximum occurrence.

Which Transmitters ?

Previous studies [*Imhof et al.* 1978, *Datlowe and Imhof*, 1989] have established that the Australian station NWC is a major source of VLF waves which resonantly interacts with trapped electrons. The transmitter UMS at 44°E has been identified by *Vampola*

and Kuck [1978] as another source of waves which pitch angle scatter electrons. It is evident from Figure 8 that as GRO moves from west to east past both of these longitudes there is a significant increase in the occurrence of electron events. The longitude distribution of events is shown in Figure 10. Out of a total of 563 events, 45 are in the longitude range of 40°E-60°E near the conjugate point of UMS, which is the probable source of VLF waves for these events. In the vicinity of NWC events are five times more frequent in this data set -- from 100°E-147°E there are 257 events. There is another block of 177 events at longitudes from 240°E to 280°E. These electrons may have undergone cyclotron resonance interactions at these longitudes or they may also have scattered at the in the eastern hemisphere and have drifted ~120° in longitude to the point of observation. The remaining 84 encounters with quasi trapped electrons occurred at other longitudes, primarily between 219° E and 240° E.

We can identify the transmitters which are the source of the quasi trapped electrons in the western hemisphere by asking where is it nighttime when these electrons are detected. Figure 11 shows the local time distribution of 257 events detected near the transmitter at NWC and the 177 western hemisphere events. In this Figure the clocks are set to local time at 114°E, which is UT + 7.6 hours. The plot shows the calculated time of injection, which is the time of injection minus the time it takes a 175 keV electron to drift from 114°E to the point of observation at 1.6° per minute. There is a good similarity between the two distributions, indicating that most of the western hemisphere events have drifted from an interaction point near NWC. Since the transmitters near 260°E are in daylight during much of this time interval, it is unlikely that they contributed significantly to the 257 occurrences of quasi trapped electrons. There is an

excess of events in the western hemisphere after 6:00 at NWC, suggesting an additional source westward of that station.

In summary, the quasi-trapped from the Australian transmitter NWC dominate the statistics, and here is good evidence that UMS is responsible for about 20% of the quasi-trapped electron encounters.

Seasonal Variation in the Frequency of Occurrence

It has been suspected from previous experiments, S81-1 and OV1-19, that there may be a seasonal variation in the frequency of occurrence of peaks. A seasonal variation in the median energy of the observed peaks was found by *Imhof et al.* [1978] in the period from November 1971 to August 1972; the energies of the peaks were reported to be lower in the summer months. The data from OV1-19 reported by *Vampola and Kuck* [1978] showed a sharp decrease in the number of observations in which cyclotron resonance effects were observed after day 270 of 1969. Plotting the S81-1 data in the same format, Datlowe and Imhof [1990] showed that the peaks in the eastern hemisphere (over NWC) were found mainly from May to September, while peaks from stations in the western hemisphere were observed primarily after September. They used the term"Seasonal Variation", although the data covered only seven months. Datlowe and Imhof [1993] used P78-1 satellite data acquired over the 5 year period from March 1979 to July 1984 to study cyclotron resonance peaks. Binning the data into seasons, they found that the events occur 2.5 times more often during the six months from day 80 to 263 than during the other six months of the year, and that the seasonal difference is statistically significant at a high level. Since the observed change is in the frequency

of occurrence of the peaks and not in the mean energy of the peaks, they attributed the effect to a seasonal change in ionospheric transmission of VLF waves rather than a seasonal change in the equatorial cold plasma density. Despite the long time span, the analyzed P78-1 data was very sparse, the time span was weighted toward the first year of operations, and the data set consisted of only 221 events. With the BATSE data we have the the advantage of 100% coverage for all but the last few days of the data used in this investigation.

We use the same format as *Vampola and Kuck* [19787, Fig. 5] and Datlowe and Imhof [1989, Fig. 13]. Like the previous studies, we assume that the transmitters are steady sources of VLF waves, operating continuously except for maintenance times; therefore they are not the origin of any time variations we observe. Figure 12 presents the results. The resonance precipitation events run in three longitude bands corresponding in sequence to UMS at 44°E, NWC at 114°E, and to events which have drifted from the eastern hemisphere to the day side of the earth. The dashed lines again delineate the 45 day period of the precession of the plane of the GRO orbit. The following is evident from the Figure:

1. The events around 114°E (NWC) were much more frequent from June 1991 to October 1991.

2. The events near 50°E (UMS)occurred primarily between August 1991 and February 1992.

3. There were very few events in December, 1991.

With the BATSE data the cyclical variation is visible in the plot, and need not be dug out by statistical tests as in the P78-1 results of *Datlowe and Imhof* [1993].

Local Time at the Transmitter Site

This BATSE data has provided the first opportunity to study the local time dependance of cyclotron resonance interactions between trapped electrons and waves from large VLF transmitters; much of the pre-existing information came from sun-synchronous satellites. Since we have continuous coverage in the first 11 months, and since the time interval is long compared to the 45 day precession period of the orbital plane, we do not need to correct for variations in the coverage. Figure 11 shows the distribution of injection times in the longitude range near NWC. By injection time we mean that a correction has been made for the time it takes an electron to drift from the transmitter site to the longitude of the satellite when the observation is made. It is clear that the events are strongly peaked the range 2:00 to 6:00.

Helliwell [1965] studied 18.6 KHz narrow band transmissions from Jim Creek, Washington, with a receiver at Stanford, Ca. These were two hop echoes -- signals that had propagated to the southern hemisphere and returned. The diurnal variation in these echoes [*op. cit.* Fig 5-13] peak before sunrise and we find them very similar to the distribution in our Figure 11. The VLF wave energy is absorbed and reflected by the ionosphere. We infer from the similarity of the VLF echoes diurnal variation and the

cyclotron resonance diurnal variation that ionospheric transmission is the controlling factor. We conclude that the resonance interactions occurred most often in the hours before sunrise because that is the time when upward propagating VLF waves have best access to the magnetospheric interaction region.

Influence of Large Geomagnetic Storms

GRO encounters with fluxes of electrons scattered by VLF transmitters typically last about 5 minutes. However, extremely narrow events have been found at times after two large geomagnetic storms. Figure 13 gives an example. from July 14, 1991, some 18 hours after the peak Kp = 9- of a geomagnetic storm [*Coffey*, 1991]. Moderate auroral x-ray emission is still evident was most visible at longitudes ~93°E and ~266°E. A pair of exceptionally narrow cyclotron resonance peaks was detected at longitudes just east of the station at NWC. In crossing each sheet of electrons the satellite moved northward only 0.12° of latitude; therefore we can estimate that the sheets were ~10 km wide. Thirty minutes later the satellite passed in reverse order through the same population of electrons which had drifted eastward to 229°E and 234°E respectively. The comparison of the two passages through these sheets of electrons is summarized in Table 1. It is evident that the calculated L-values match to within the precision of the calculation and the two second time resolution of the data. The intensities also compare very well between eastern and western hemispheres, although there is a differences in the equatorial pitch angles.

Table 1

UT	Longitude degrees E	L	Eq. P.A. degrees	Rate >50 keV	Duration seconds
39197	122.3	1.555	28.0	39420	12
41149	233.9	1.554	31.3	30978	12
39254	125.8	1.505	29.8	74242	10
41081	229.4	1.500	33.7	81831	10
46916.	221.8	1.520	33.1	199522	192

Because we have a limited number of energy channels and because we measure x-rays and not the electrons directly, the spectrum of the electrons is not observed. But we know from the fact that the pitch angle scattering is resonant according to equation (1) that the spectrum of electrons is also narrowly peaked. Based on the L-value of 1.5 we estimate the energy of the peak to be 300 keV [*Datlowe and Imhof*, 1990, appendix]. The counting rate data shows significant counts above 100 keV but nothing in the 300 keV channel.

The second event of this type occurred on 22 November, 1991 at an L-value of 1.40, following a geomagnetic storm with Kp = 5.

The origin of such a narrow ~10 km interaction region is a puzzle. We know that regions of VLF wave injection can extend hundreds of km around a transmitter site [*Inan et al.*, 1984] and that the magnetic field in the inner magnetosphere is smooth.

Only a sharp feature or gradient in the cold plasma density can provide such a localized region in which the resonance condition is met. In this regard we note that the ducts of enhanced plasma density inferred from whistler observations [*Helliwell* 1965 p 134] are of this same size scale.

Summary

We have identified 563 instances in which the Compton Gamma Ray observatory traversed a cloud of energetic electrons which has been scattered into quasi-trapped trajectories by waves from a large VLF transmitter. By proximity to the transmitter at nighttime, we conclude that waves from the VLF transmitter NWC at 114°E are the origin of 257 of the events, and waves from UMS at 44°E related to 45 more. The remaining 177 have drifted from these transmitter to a location in the western hemisphere. We find no unambiguous evidence for contributions from other VLF stations. The previously reported seasonal variation in the frequency of occurrence of cyclotron resonance interaction is confirmed with the continuous coverage provided by GRO. The diurnal variation in the frequency of occurrence of the quasi-trapped electron fluxes is similar to the diurnal variation of VLF echoes and like the echoes we attribute the origin of the effect to diurnal variations in the transmission VLF waves through the ionosphere. We also report for the first time unique very narrow sheets of electrons occurring in the aftermath of a large geomagnetic storm.

Acknowledgments

This work was carried out under the Compton Gamma Ray Observatory Guest Investigator program under contract NAS5-32065. The help of Jay Norris and Sandy Barnes of the GRO Science Support Center at Goddard Space Flight Center is greatly appreciated. Mark Finger kindly provided the BATSE DISCLA data on 8mm tapes. Finally, the support and encouragement of Gerald Fishman was crucial to this investigation.

APPENDIX

The **geomagnetic coordinates** of a satellite when it is 450 km over the stations marked in Figure 7 are as follows:

STN	FREQ kHz	POWER KW	LAT	LONG	L	CONJ Km
NAA	17.8	1000.	44.7	292.7	3.28	105.
NLK	24.8	850.	48.2	238.1	3.10	742.
NPM	23.4	300.	21.4	201.9	1.22	726.
NSS	21.4	265.	39.0	283.6	2.68	347.
NWC	22.3	1000.	-21.8	114.2	1.46	573.
GBR	16.0	300.	52.3	0.3	2.59	-597.
UMS	16.2	1000.	56.	44.	2.79	62.
RPS	17.1	1000.	43.	135.	1.55	760.
Siple	var	3.	-75.9	275.8	4.70	1077.

Station location, frequency and power from

Inan, U. S., H. C. Chang, and R. A. Helliwell, Electron precipitation zones around major ground-based VLF signal sources, *J. Geophys. Res. 89*, 2891, 1984

The calculation of geomagnetic coordinates based on

Olsen, W. P., and K. A. Pfitzer, A quantitative model for the magnetospheric magnetic field, *J. Geophys. Res. 79*, 3739, 1974

9 February, 1994

Figure Captions

Figure 1

Equatorial pitch angle of electrons mirroring at 200 km. The solid line shows electrons mirroring in the southern hemisphere and the dashed line electrons mirroring in the northern hemisphere. Between 270° (90° W) and 63°E electrons in the northern hemisphere have a conjugate point below 100 km and will be absorbed within a few bounce periods (~1 sec). A satellite with a 28.5° orbital inclination reaches L=1.65 only between 6°E and 147°E in the south and between 258°E and 309°E in the north.

Figure 2

BATSE DISCLA counting rate above 50 keV on June 24, 1991 from 14:18 UT to 15:57 UT. The upper trace is the sum of the 8 detectors, and the scaling is given on the left axis. The lower trace shows σ as defined in the text and the scale from .01 to 1.0 on the right axis. The horizontal scale is in degrees, and the satellite moves from left to right at 3.6° per minute. The peak occurs was observed at 144°E at L= 1.61 .

Figure 3

BATSE DISCLA counting rate above 50 keV three orbits later, covering the time interval 19:17 Ut to 20:58 UT. The peaks are located at 131.9°E (L= 1.68) and 250.7°E (L = 1.66).

Figure 4

BATSE DISCLA counting rate during times of auroral emission above 50 keV. At this time on 2 June 1991 the three hour average of Kp was 6- [*Coffey*, 1991]. The first event was BATSE trigger #203.

Figure 5

BATSE DISCLA counting rate above 50 keV from a solar flare on 17 June 1991. The flare was classified by the GOES satellite as class M (BATSE trigger #203).

Figure 6

BATSE DISCLA counting rate above 50 keV on April 29, 1991. The plot shows successively an auroral event (BATSE trigger # 120), a true cosmic x-ray burst (trigger # 121) and quasi trapped electrons (trigger #122). The peak of the electrons event was observed at longitude 268°E . The inset shows the x-ray burst at higher time resolution, 100 s full scale [from *Fishman et al.* 1994]

Figure 7

A geographic map of the locations of the 563 electron precipitation events. The number of events in each 5°x5° bin is displayed on the gray-scale at the lower right. The nothern and southern contours of L=1.65 at 450 km altitude are solid lines. Transmitters are indicated in the Figure by • and are listed in the Appendix.

Figure 8

Equatorial pitch angle for the peaks of 189 events which occurred between L=1.60 and L=1.70 as a function of longitude. The equatorial pitch angle of electrons mirroring at 200 km is plotted as a solid line (south) or dashed line (north) at longitudes where L=1.65 is reachable by a 28.5° inclination orbit.

Figure 9

Counting rate above 50 keV at the peak of all the electron events as a function of time. The time axis is marked in day-of-year, starting on 24 April 1991 and ending 26 April 1992.

Figure 10

Longitude distribution of the 563 GRO encounters with energtic electrons scattered into quasi trapped orbits by cyclotron resonance with VLF waves. In each case the longitude of the highest BATSE couting rate is plotted.

Figure 11

The number of times BATSE recorded electrons in quasi trapped orbits versus the local time at 114 °E (longitude of NWC).

Upper: 177 Events in the longitude range 240°E to 280°E.

Lower: 247 Events from 100°E to 147°E

Figure 12

The occurrence of transmitter induced precipitation events as a function of time (season) and East longitude. The observations have been sorted into bins of 15 °E longitude by 9 days. The number of times cyclotron resonance precipitation electrons were detected is gray-scale coded from 1 to a maximum of 15 events in 9 days. For comparison, the satellite crosses any given meridian 14.4 times per day. The 45 day precession period of the plane of the satellite orbit is the time interval between the dashed lines. The vertical axis is labelled in day-of-year from 24 April 1991 to 26 April 1992.

Figure 13

The very narrow transmitter precipitation events on 14 July, 1991. The plot shows two consecutive orbits of data. The arrows indicate the following:

A) Two ~10 km sheets of trapped electrons which the satellite crossed at 39197 UT and 39254 UT respectively.

B) The same electron population which as drifted from ~93°E to ~232° E.

C) Trapped electrons observed in the south Atlantic anomaly

D) A broad peak of electrons which have drifted from the transmitter site to the western hemisphere.

E) X-ray emission from the southern and northern auroral zones.

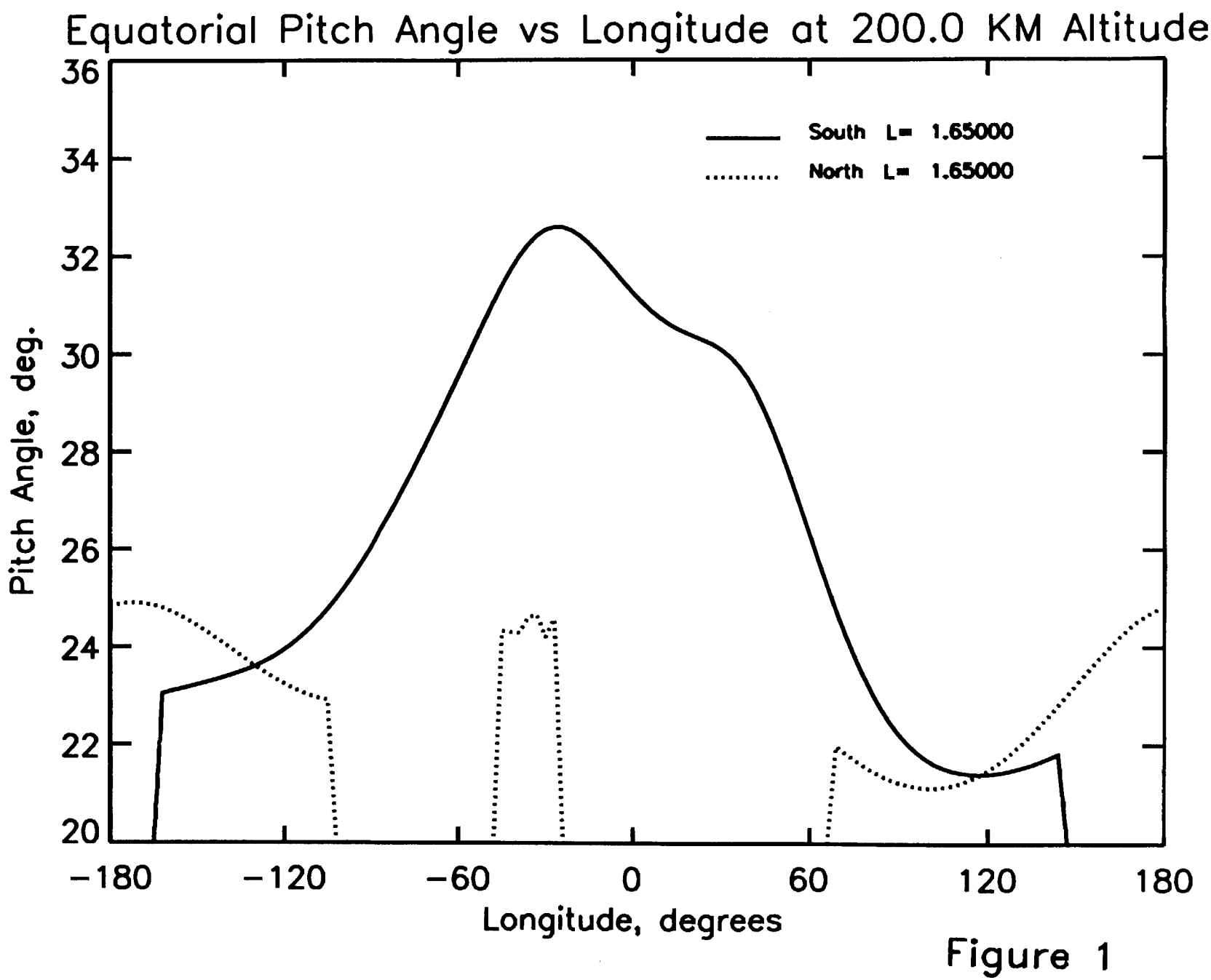
Equatorial Pitch Angle vs Longitude at 200.0 KM Altitude
South L= 1.65000
North L= 1.65000
Pitch Angle, deg.
36
34
32
30
28
26
24
22
20
−180
−120
−60
0
60
120
180
Longitude, degrees

Figure 1

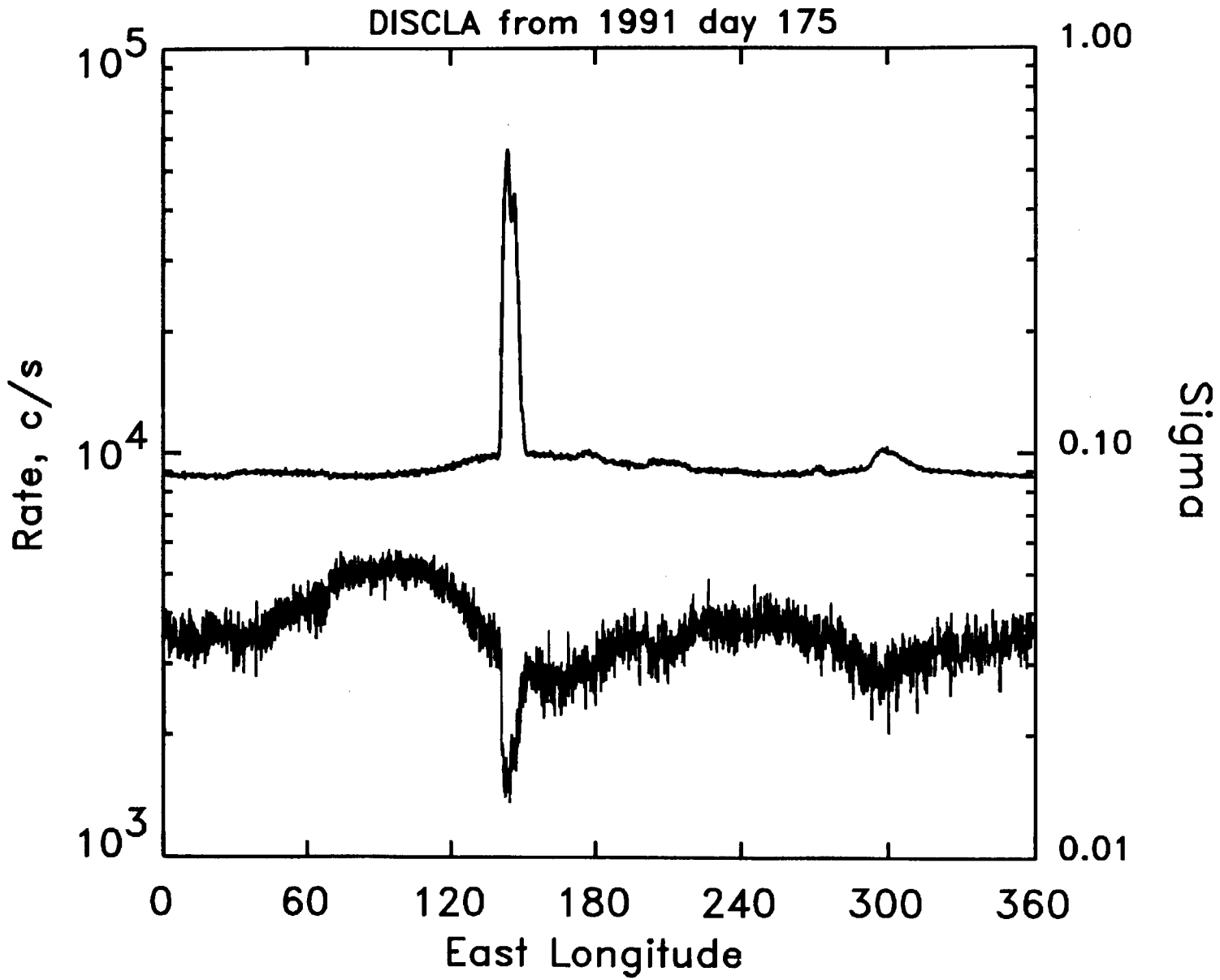
DISCLA from 1991 day 175
10^5
10^4
10^3
Rate, c/s
1.00
0.10
0.01
Sigma
0
60
120
180
240
300
360
East Longitude

Figure 2

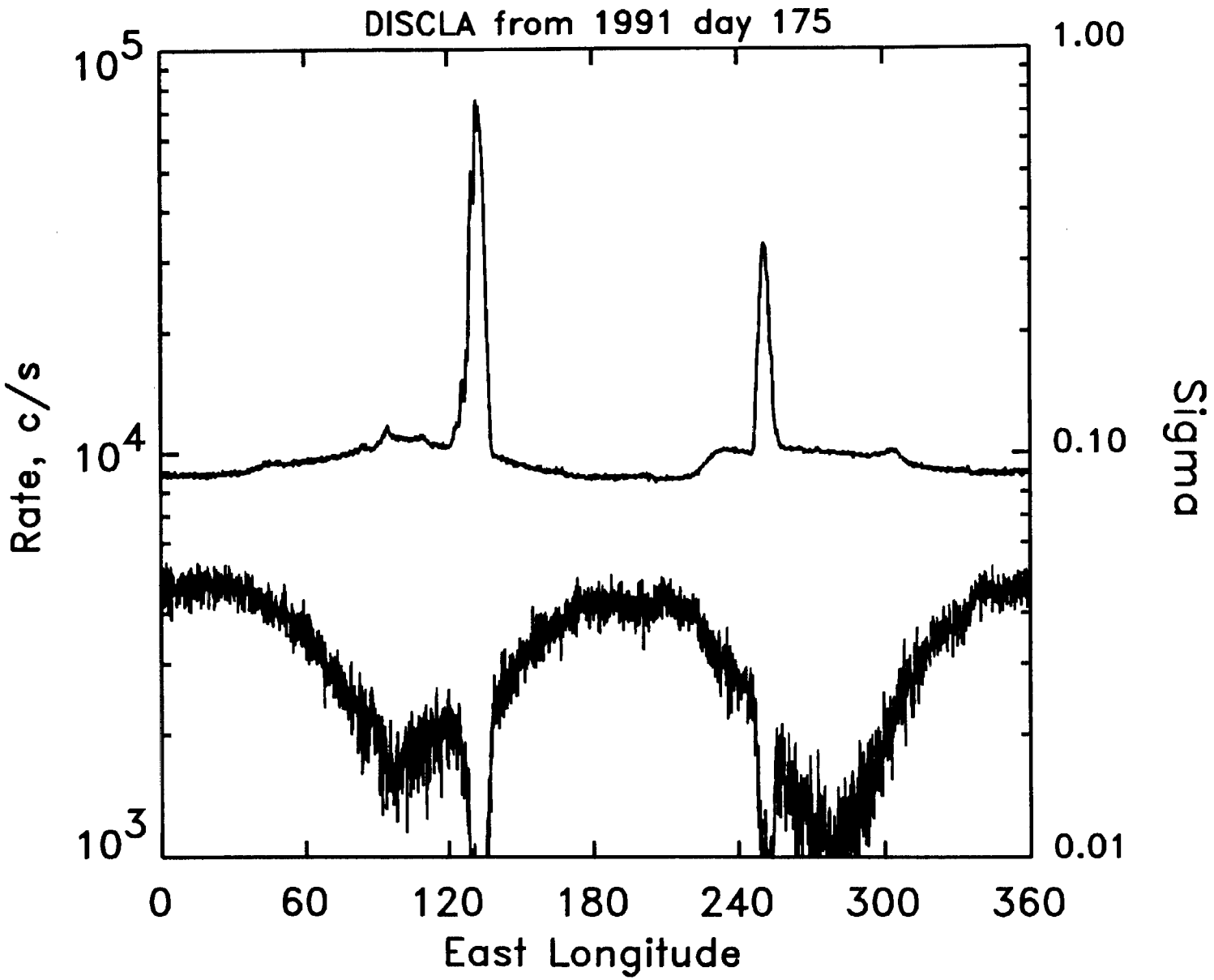
DISCLA from 1991 day 175
10^5
10^4
10^3
Rate, c/s
1.00
0.10
0.01
Sigma
0
60
120
180
240
300
360
East Longitude

Figure 3

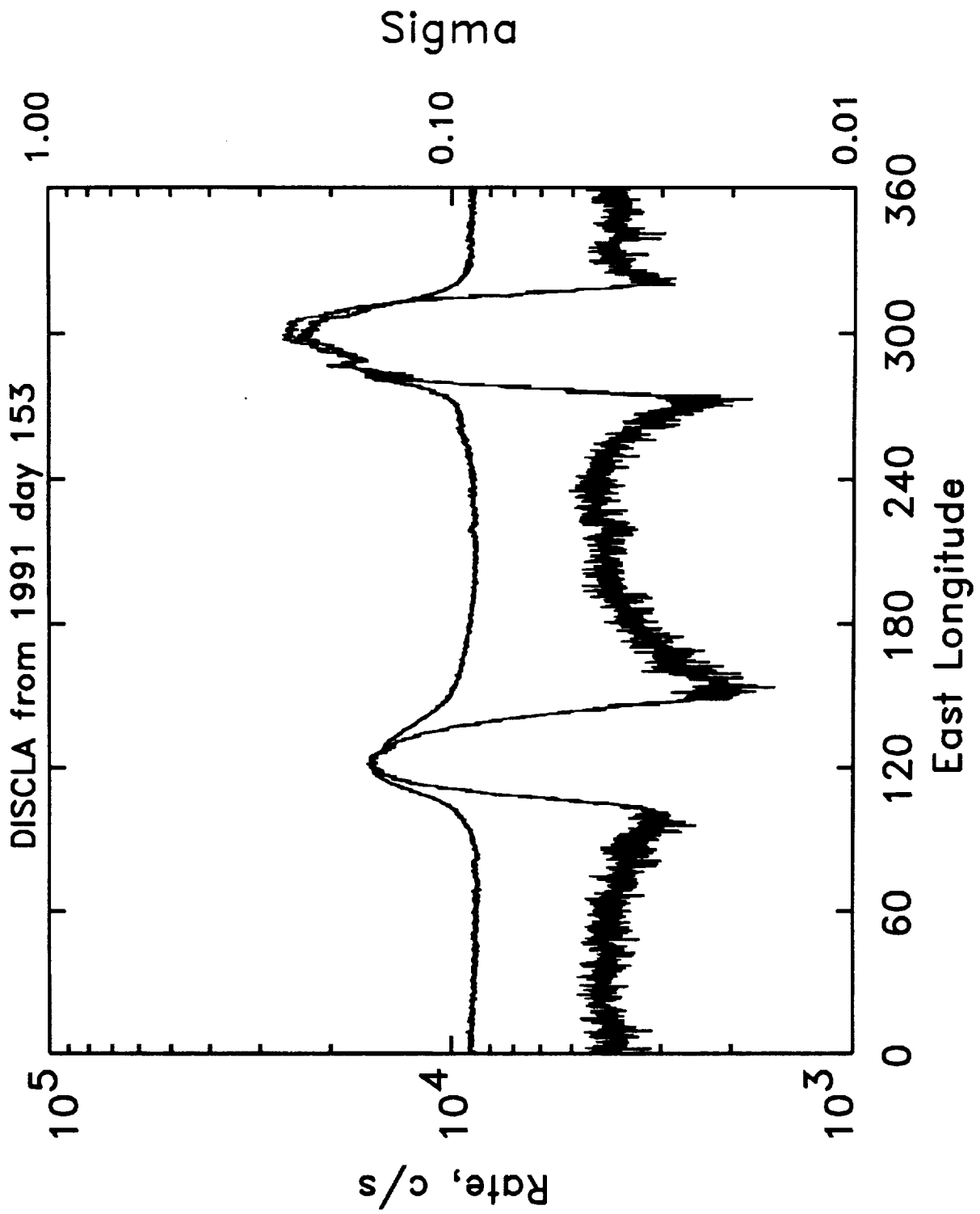
Sigma
1.00
0.10
0.01
DISCLA from 1991 day 153
10^5
10^4
10^3
Rate, c/s
0
60
120
180
240
300
360
East Longitude

Figure 4

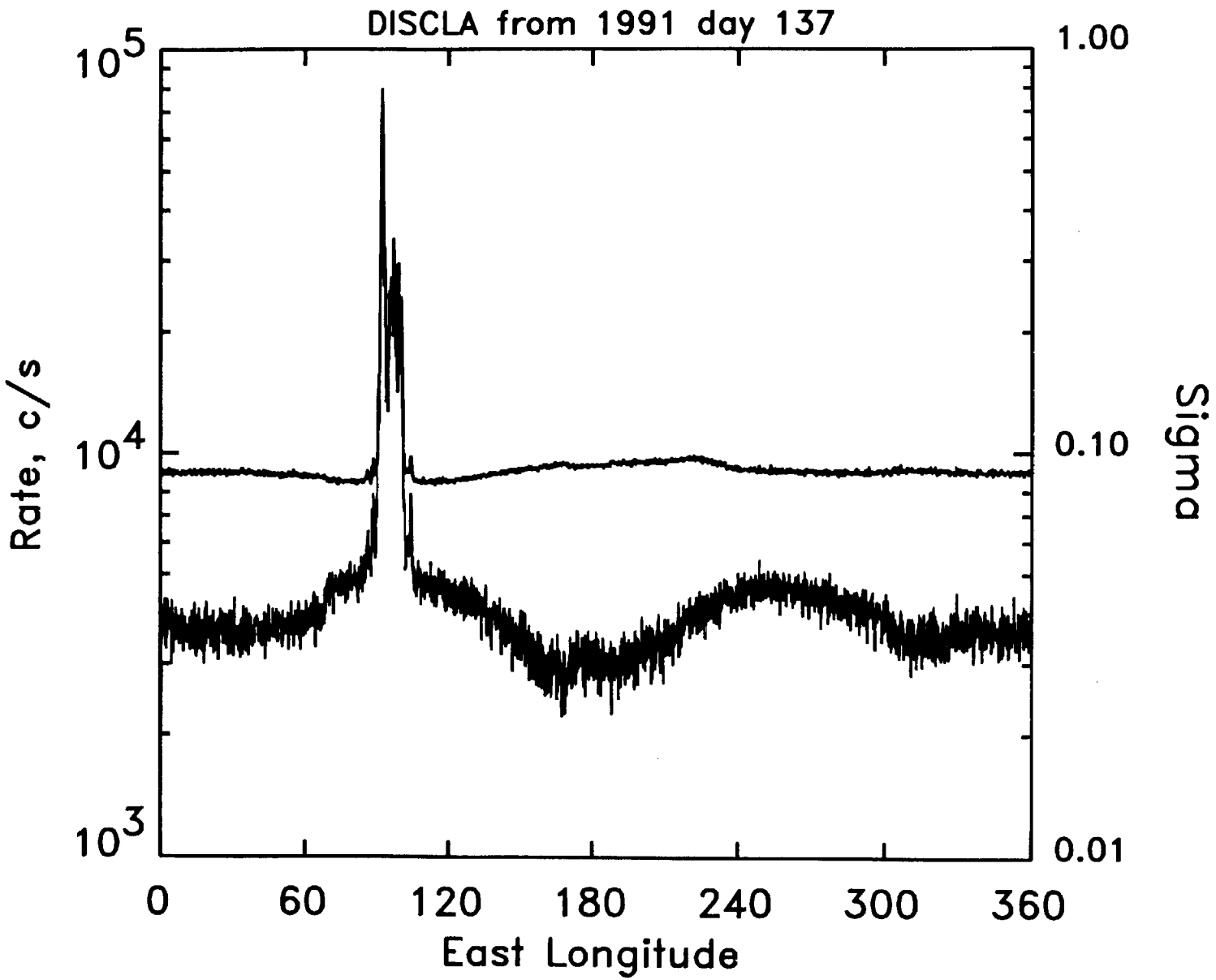
DISCLA from 1991 day 137
10^5
10^4
10^3
Rate, c/s
1.00
0.10
0.01
Sigma
0
60
120
180
240
300
360
East Longitude

Figure 5

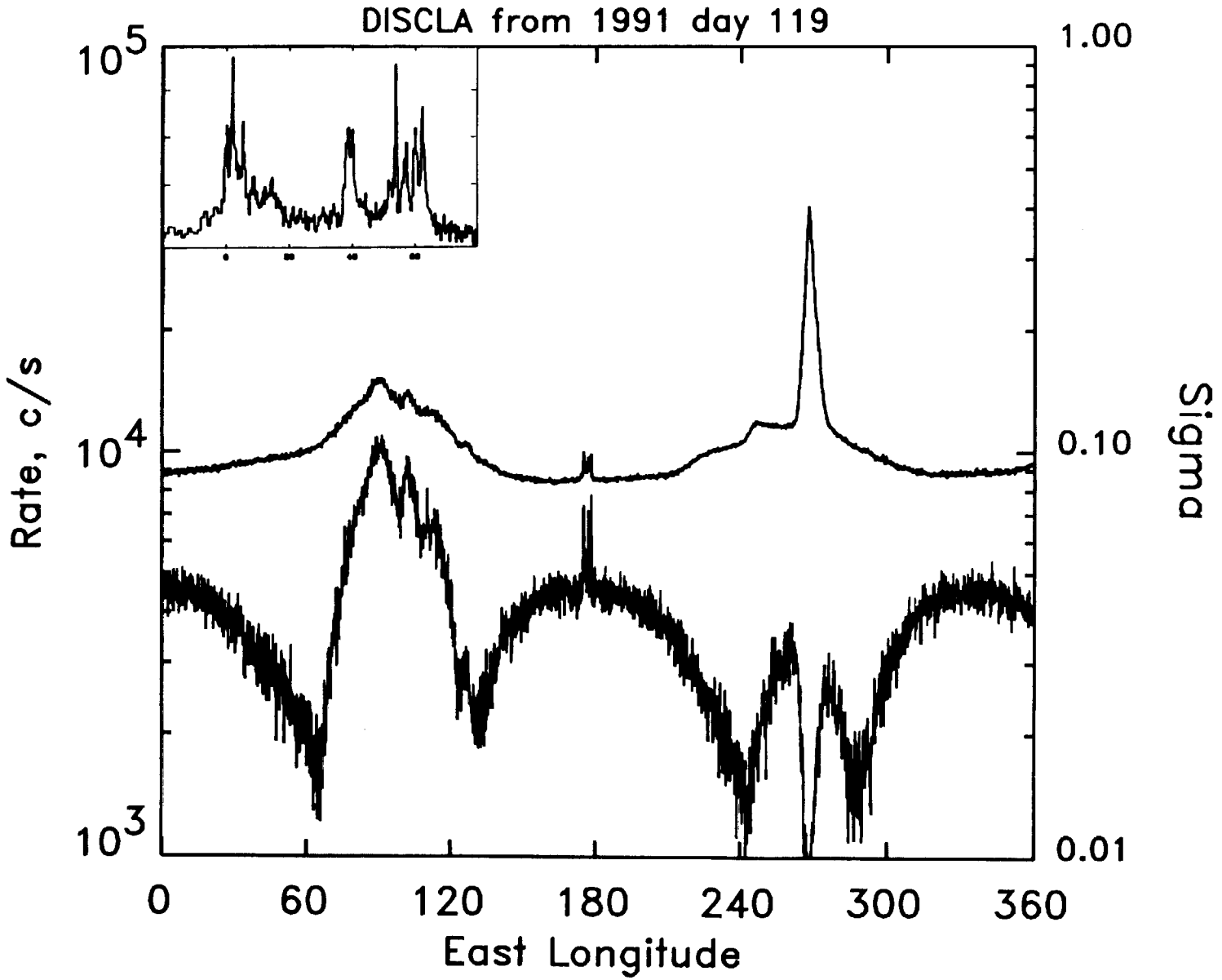
DISCLA from 1991 day 119
10^5
10^4
10^3
Rate, c/s
1.00
0.10
0.01
Sigma
0
60
120
180
240
300
360
East Longitude

Figure 6

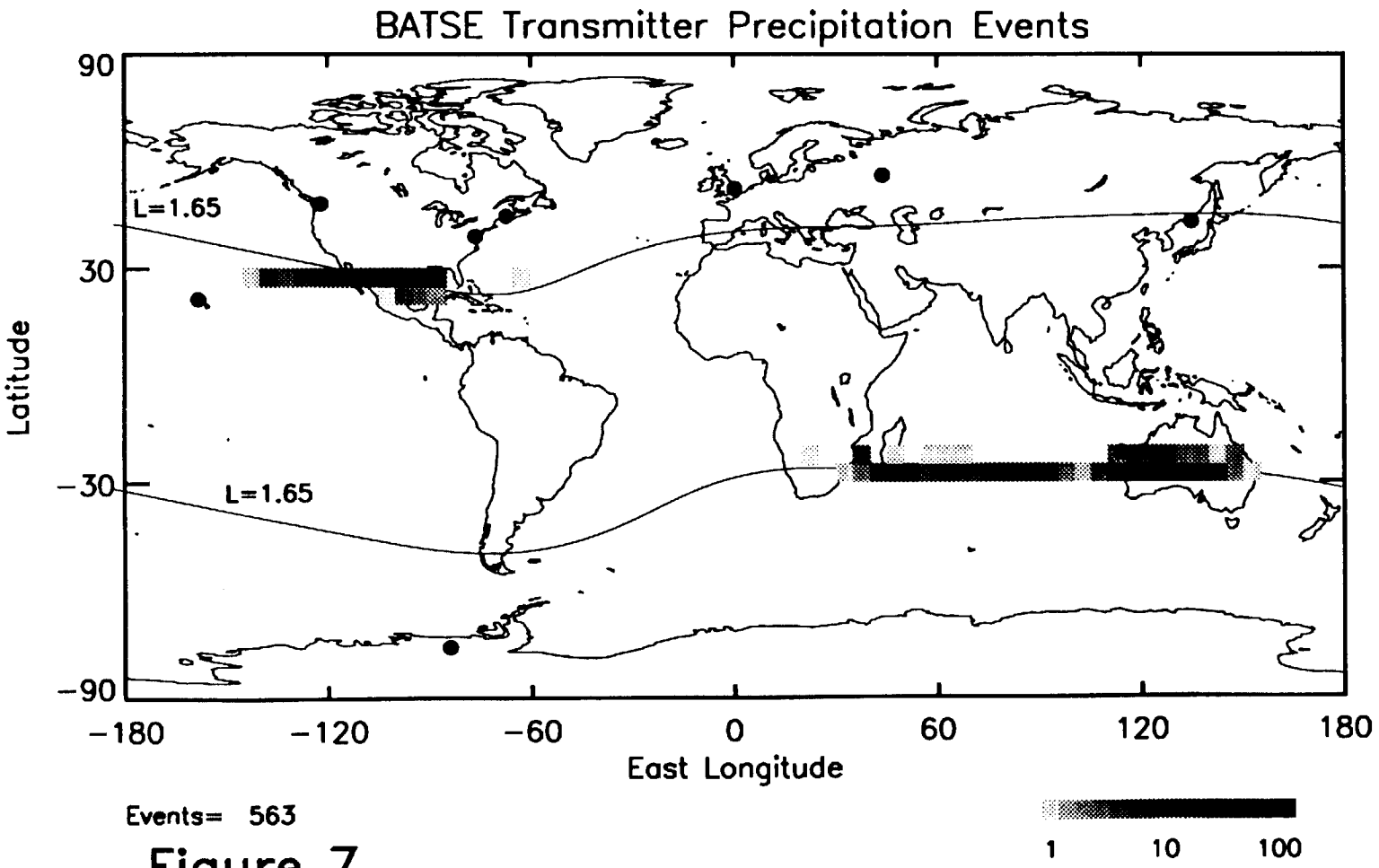
BATSE Transmitter Precipitation Events
90
30
−30
−90
Latitude
L=1.65
L=1.65
−180
−120
−60
0
60
120
180
East Longitude
Events= 563
1
10
100

Figure 7

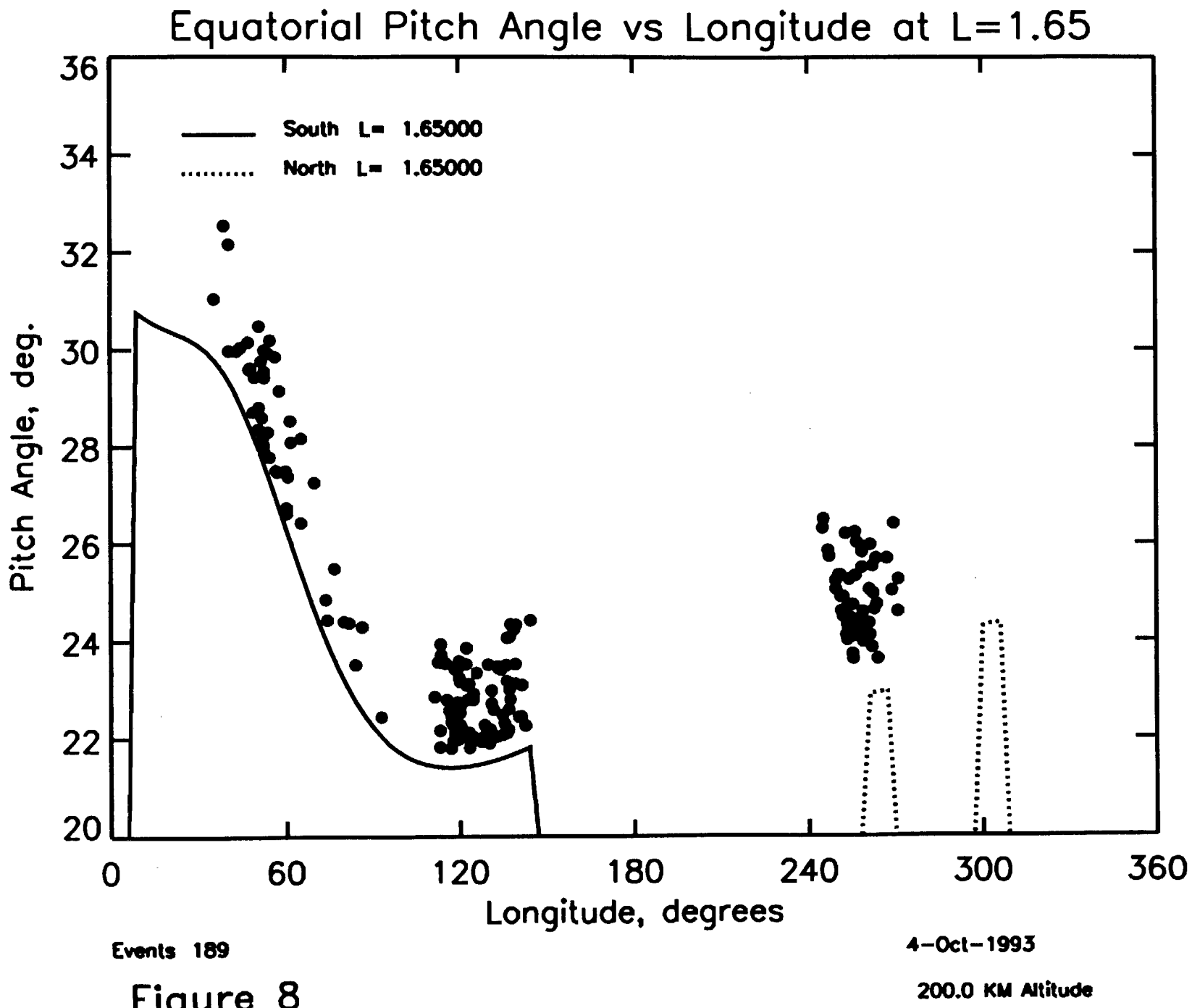
Equatorial Pitch Angle vs Longitude at L=1.65
South L= 1.65000
North L= 1.65000
Pitch Angle, deg.
36
34
32
30
28
26
24
22
20
0
60
120
180
240
300
360
Longitude, degrees
Events 189
4-Oct-1993
200.0 KM Altitude

Figure 8

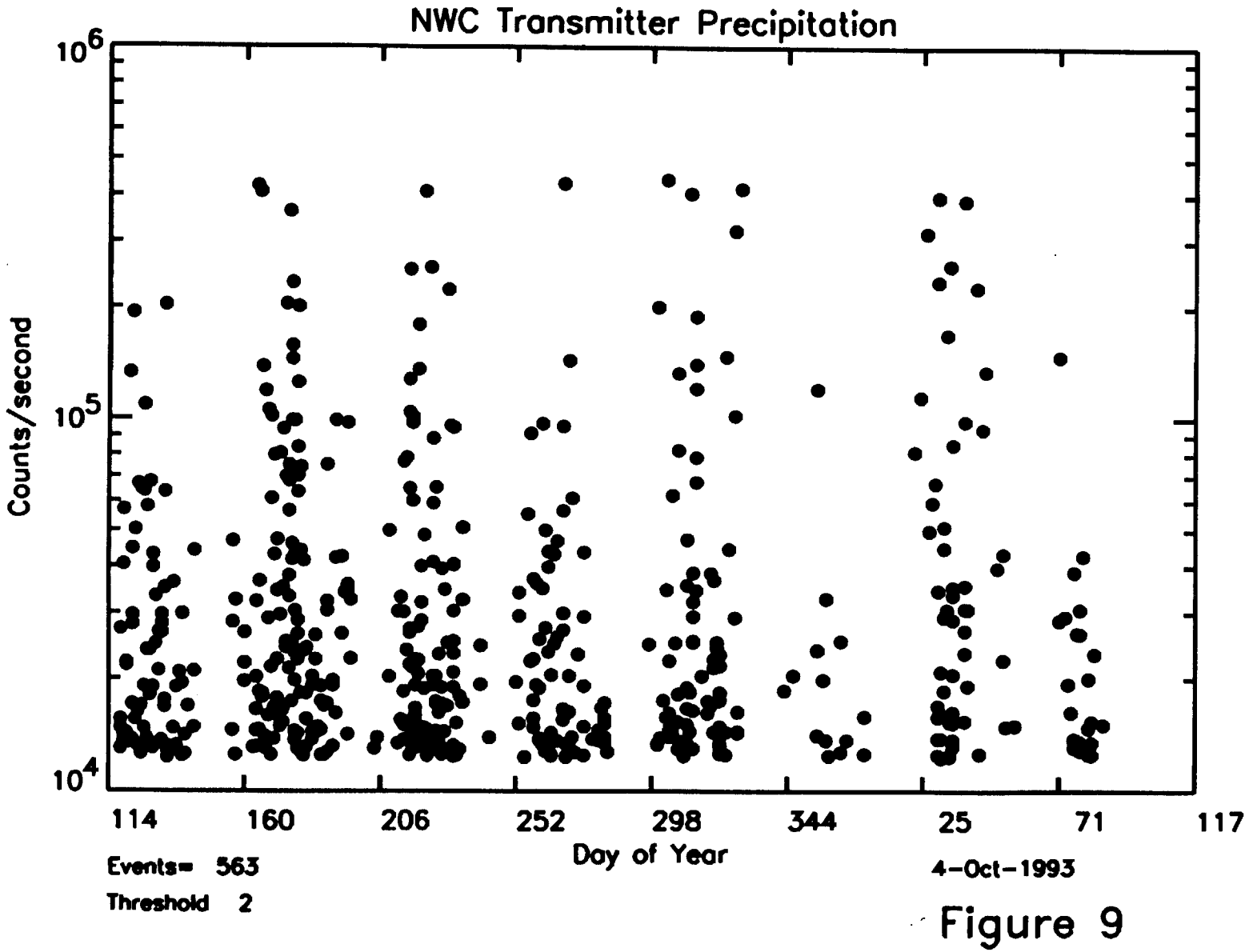
NWC Transmitter Precipitation
10^6
10^5
10^4
Counts/second
114
160
206
252
298
344
25
71
117
Day of Year
Events= 563
Threshold 2
4-Oct-1993

Figure 9

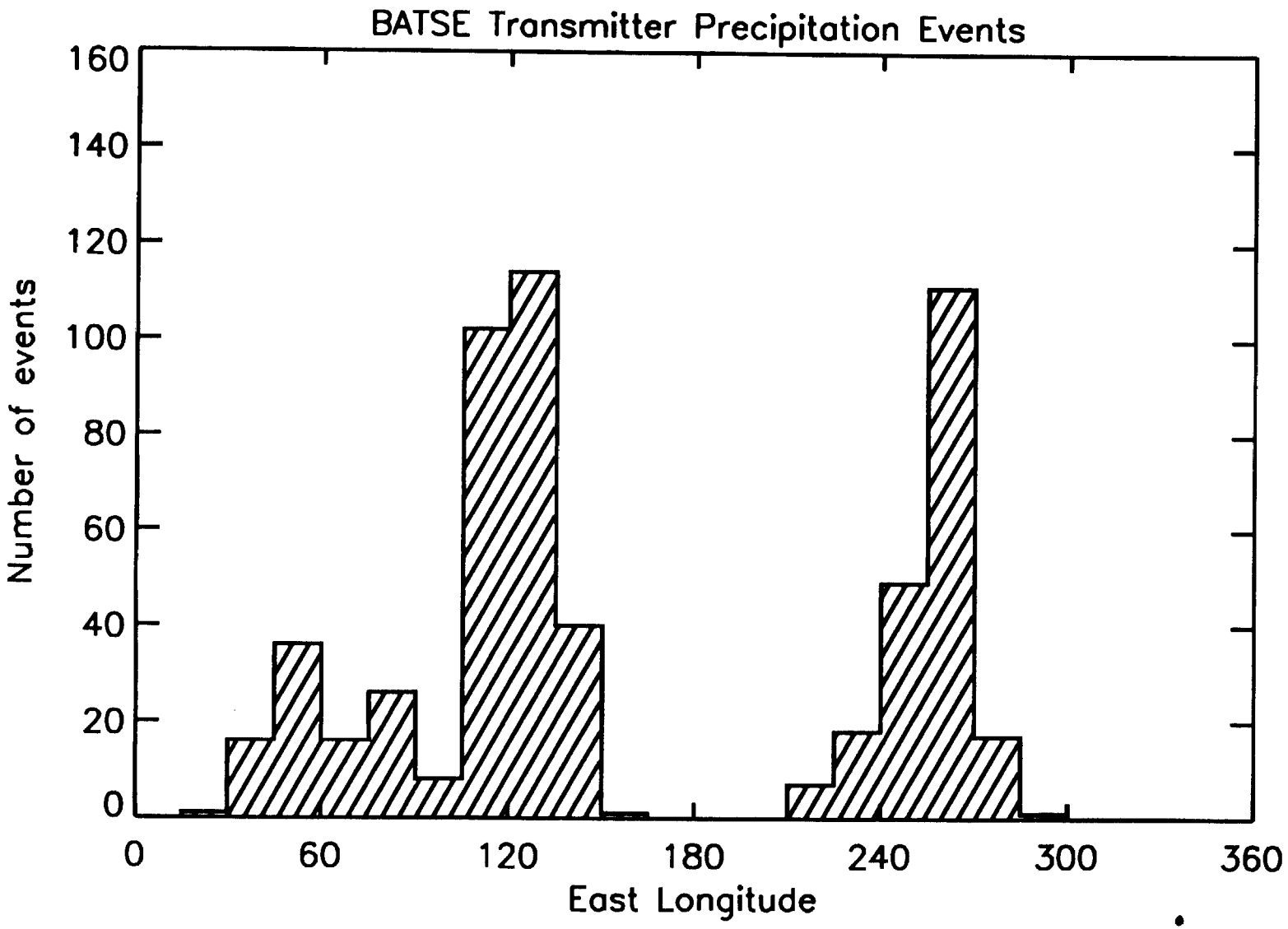
BATSE Transmitter Precipitation Events
160
140
120
100
80
60
40
20
0
Number of events
0
60
120
180
240
300
360
East Longitude
Events= 563

Figure 10

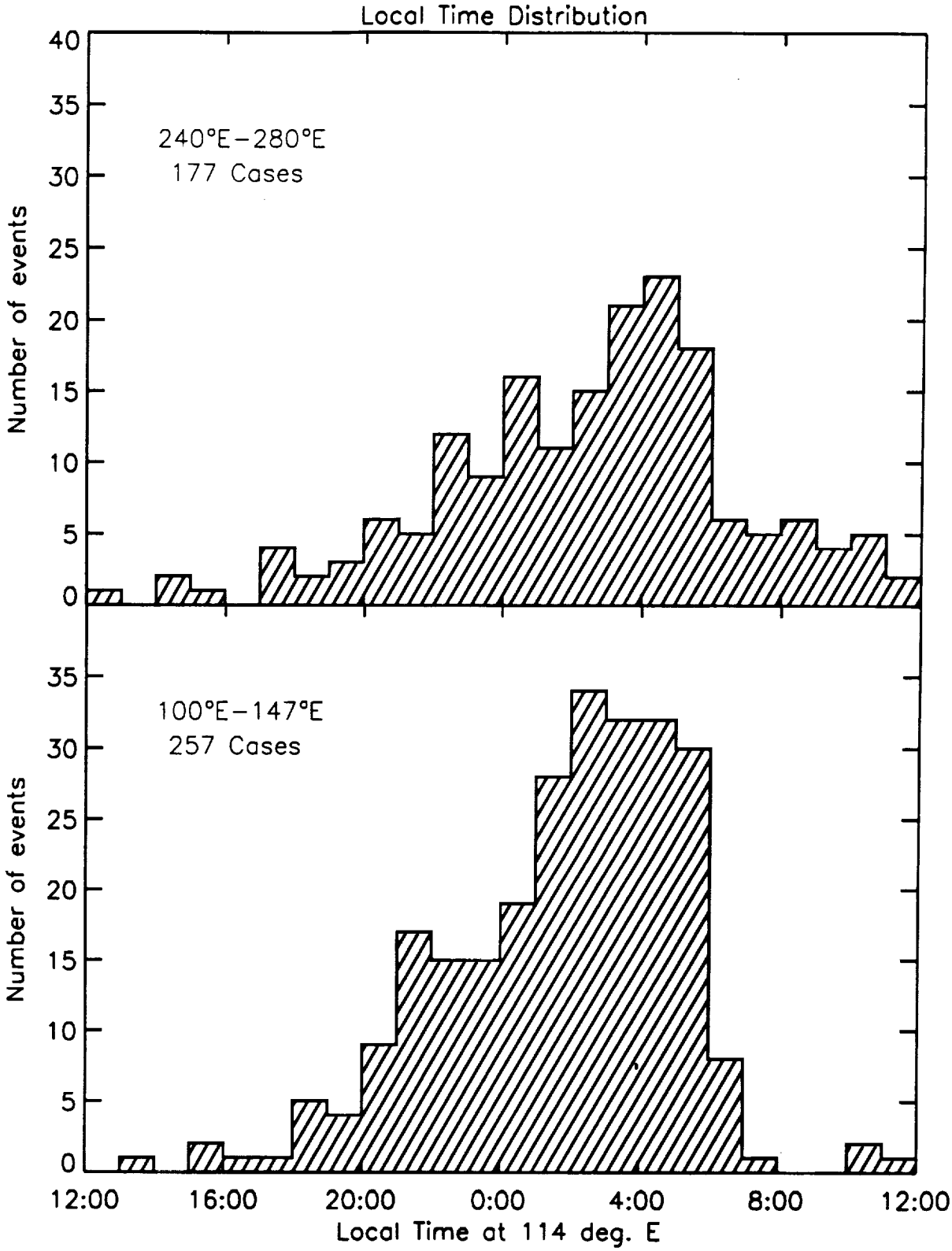
Local Time Distribution
240°E–280°E
177 Cases
100°E–147°E
257 Cases
Number of events
Number of events
0
5
10
15
20
25
30
35
40
12:00
16:00
20:00
0:00
4:00
8:00
12:00
Local Time at 114 deg. E

Figure 11

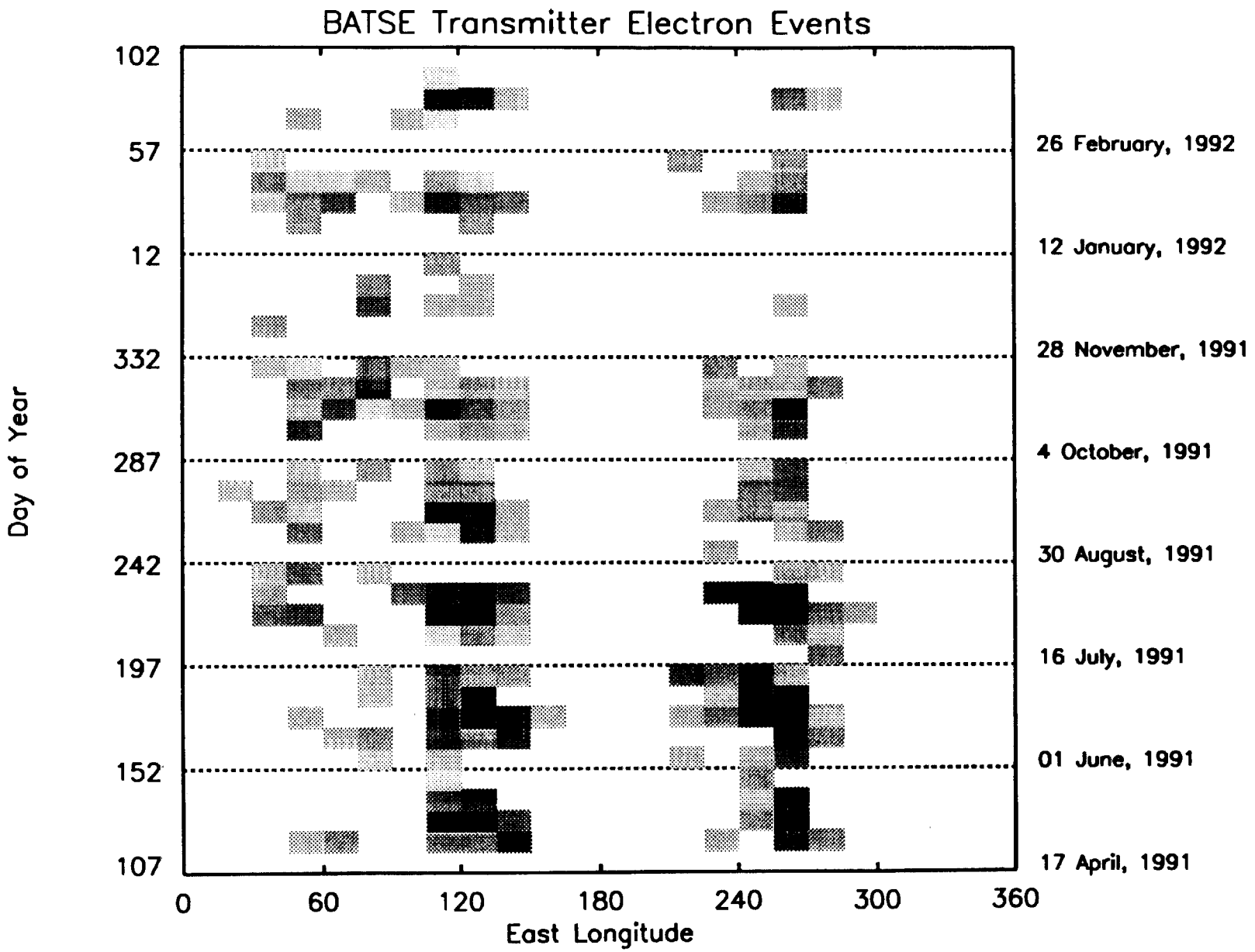
BATSE Transmitter Electron Events
102
57
12
332
287
242
197
152
107
Day of Year
26 February, 1992
12 January, 1992
28 November, 1991
4 October, 1991
30 August, 1991
16 July, 1991
01 June, 1991
17 April, 1991
0
60
120
180
240
300
360
East Longitude
Events= 563
1
5
10
15

Figure 12

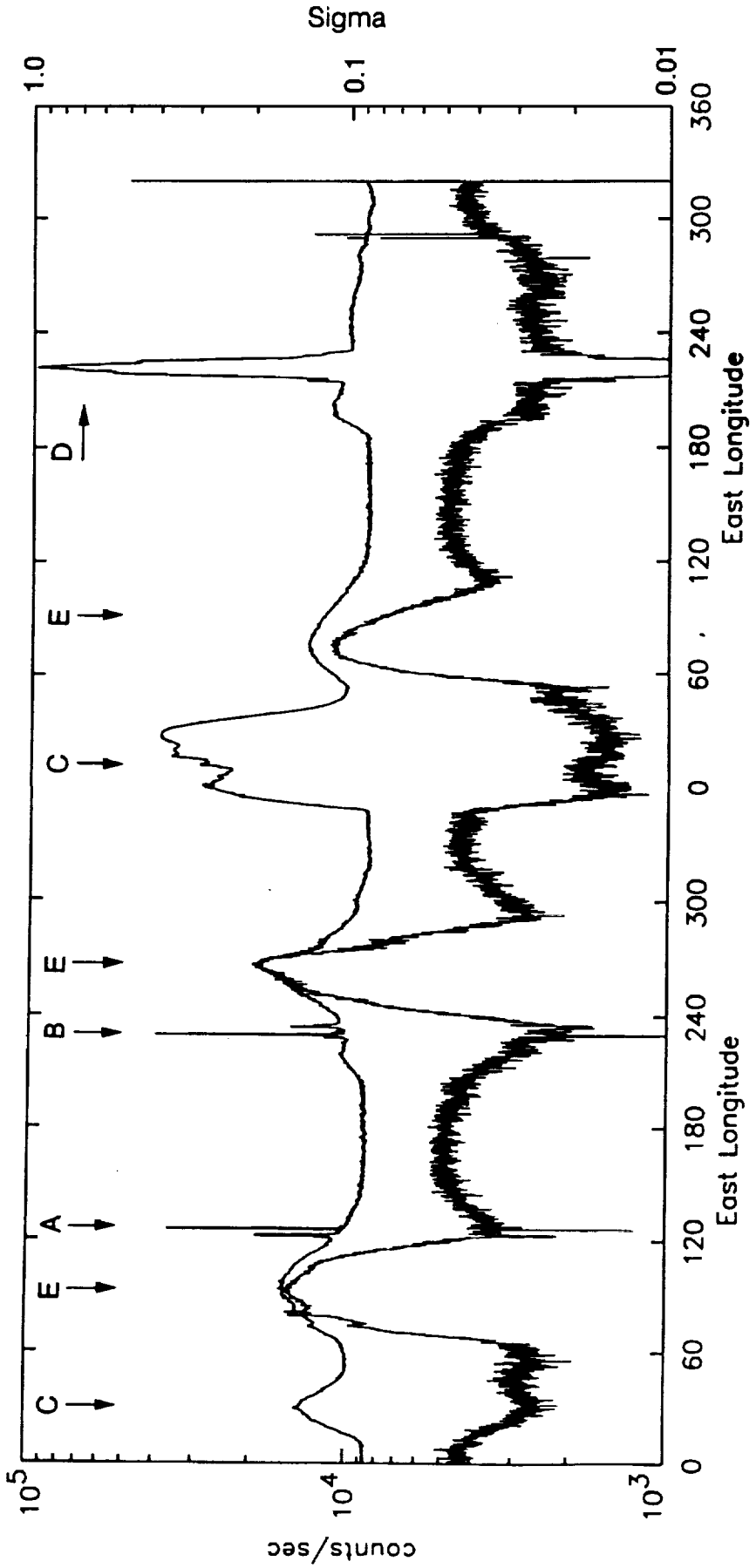
Sigma
1.0
0.1
0.01
360
300
240
180
120
60
0
East Longitude
D
E
C
E
B
E
A
E
C
10^5
10^4
10^3
counts/sec

Figure 13

REPORT DOCUMENTATION PAGE

Form Approved
OMB No. 0704-0188

1. AGENCY USE ONLY *(Leave blank)*	2. REPORT DATE	3. REPORT TYPE AND DATES COVERED
	February 1994	Contractor Report

4. TITLE AND SUBTITLE
Compton Gamma-Ray Observatory/BATSE Observations of Energetic Electrons Scattered by Cyclotron Resonance with Waves from Powerful VLF Transmitters

5. FUNDING NUMBERS
NAS5-32065

6. AUTHOR(S)
D. W. Datlowe and W. L. Imhof

7. PERFORMING ORGANIZATION NAME(S) AND ADDRESS(ES)
Space Sciences Laboratory/Research and Development Division
Lockheed Missles and Space Company 0 91-20 B 255
3251 Hanover Street
Palo Alto, CA 94304-1191

8. PERFORMING ORGANIZATION REPORT NUMBER
LMSC F254276

9. SPONSORING/MONITORING AGENCY NAME(S) AND ADDRESS(ES)
National Aeronautics and Space Administration
Washington, D.C. 20546–0001

10. SPONSORING/MONITORING AGENCY REPORT NUMBER
CR-189336

11. SUPPLEMENTARY NOTES

12a. DISTRIBUTION/AVAILABILITY STATEMENT
Unclassified–Unlimited
Subject Category 73

12b. DISTRIBUTION CODE

13. ABSTRACT *(Maximum 200 words)*

To obtain a better understanding of the wave-particle mechanisms responsible for the loss of electrons from the radiation belts, we have studied energetic electron data from the Burst and Transient Source Experiment (BATSE) on the NASA's Compton Gamma Ray Observatory (GRO). Powerful ground-based VLF transmitters resonantly scatter electrons from the inner radiation belt onto trajectories from which they precipitate into the atmosphere as they drift eastward. We have identified 563 instances in which the satellite traversed a cloud of energetic electrons which had been scattered into quasi-trapped trajectories. From the longitude distribution we conclude that waves from the VLF transmitter NWC at 114°E are the origin of 257 of the events, and waves from UMS at 44°E related to 45 more. In another 177 cases the electrons had drifted from the longitude of these transmitters to a location in the western hemisphere. The previously reported seasonal variation in the frequency of occurrence of cyclotron resonance interaction is confirmed with the continuous coverage provided by GRO. The frequency of occurrence of the cyclotron resonance interations is largest before sunrise, which we attribute to the diurnal variations in the transmission VLF waves through the ionosphere. We also report for the first time unique very narrow sheets of electrons occurring in the aftermath of a large geomagnetic storm.

14. SUBJECT TERMS
Compton Gamma-ray Observatory, Burst and Transient Source Experiment (BATSE)
Energetic Particle Precipitation, VLF

15. NUMBER OF PAGES
20

16. PRICE CODE

17. SECURITY CLASSIFICATION OF REPORT	18. SECURITY CLASSIFICATION OF THIS PAGE	19. SECURITY CLASSIFICATION OF ABSTRACT	20. LIMITATION OF ABSTRACT
Unclassified	Unclassified	Unclassified	Unlimited